Stevenson, G. T. (1973), *Biochem. J. 133*, 827.
Stevenson, G. T., and Dorrington, K. J. (1970), *Biochem. J. 118*, 703.
Strickland, E. H., Horwitz, J., and Billups, C. (1969), *Biochemistry 8*, 3205.
Titani, K., Whitley, E., Jr., and Putnam, F. W. (1966), *Science 152*, 1513.
Voss, E. W., Jr., and Eisen, H. N. (1968), *Fed. Proc., Fed. Am. Soc. Exp. Biol. 27*, 684.
Wang, B. C., and Sax, M. (1974), *J. Mol. Biol. 87*, 505.
Weber, K., and Osborn, M. (1969), *J. Biol. Chem. 244*, 4406.
Yoo, T. J., Roholt, O. A., and Pressman, D. (1967), *Science 157*, 707.
Zeppezauer, M., Eklund, H., and Zeppezauer, E. S. (1968), *Arch. Biochem. Biophys. 126*, 564.

Crystal Properties as Indicators of Conformational Changes during Ligand Binding or Interconversion of Mcg Light Chain Isomers†

K. R. Ely,‡ J. R. Firca,§ K. J. Williams, E. E. Abola,‡ J. M. Fenton, M. Schiffer, N. C. Panagiotopoulos, and A. B. Edmundson*,‡

ABSTRACT: Crystals were prepared from samples of noncovalent and covalently linked dimers previously isolated as intermediates and end products in the interconversion of conformational isomers of immunoglobulin light chains from the patient Mcg. In ammonium sulfate these dimers crystallized in the trigonal form characteristic of the native Bence-Jones protein and in an abnormal needle form associated with conformational changes in the vicinity of the interchain disulfide bond. Trigonal forms were compared with the native covalent dimer by difference Fourier analysis at 3.5-Å resolution. Criteria were established for recognizing and cutting twinned trigonal crystals into fragments useful for diffraction experiments. The packing of molecules in the trigonal crystal lattice was examined in detail to determine the steric limitations governing chemical modifications, chemical modifications within crystals or in solutions slated for crystallization. When the modifications involved only the cleavage and alkylation of the interchain disulfide bond, the difference Fourier maps indicated only local conformational changes mainly in the COOH-terminal pentapeptide segment of monomer 2 of the dimer. When light chains were dissociated from heavy chains and reassembled into a dimer, there were changes in segments which interact to stabilize the V domain dimer (i.e., in the lining of the deep binding pocket in the V interface). These changes, as well as the more extensive changes in the needle forms, could be reversed by dissolving the crystals, cleaving the interchain disulfide bond, and allowing it to reoxidize. The resulting proteins crystallized as trigonal forms indistinguishable from those of the native dimer. After the binding of two molecules of bis(dinitrophenyl)lysine and subsequent removal of the ligands by dialysis, the dimer crystallized only as needles. The needles could be converted into trigonal forms as before. These results suggest that the binding of ligands by the V domains can lead to conformational changes in the most distal regions of the C domain dimer.

In the interconversions of conformational isomers of the Mcg immunoglobulin light chains (see Firca et al., 1978), we initially considered crystallization of the products to be just a routine step in the correlation of chemical and diffraction results. Instead, the unexpected appearance of different crystal forms and variations in the properties of the expected crystal forms directed us into a more enlightened study of conformational changes in the constituent molecules. By using the crystal properties in conjunction with chemical modifications and CD spectroscopy (see Firca et al., 1978), we were able to identify regions involved in conformational changes during the interconversion experiments. The morphology and pertinent properties of these crystals will be described in the present article. In cases in which the crystal morphology was similar to that of the trigonal form of the native Bence-Jones dimer (Edmundson et al., 1971), subtle conformational changes were studied in detail by difference Fourier analysis. The crystal packing in the trigonal form was examined to determine what changes were possible without destruction of the lattice.

The presence of other crystal forms was taken as evidence of more substantial conformational differences, as shown in solution by the comparisons of the CD spectra of trigonal and needle forms. Information on the nature of the latter differences was obtained from the procedures required to convert the altered molecules into species crystallizing like native dimers.

In contrast to the results for the New and McPC 603 Fab fragments (Amzel et al., 1974; Poljak et al., 1974; Segal et al., 1974; Davies et al., 1975; Padlan et al., 1976), local conformational changes can be induced by the binding of some hapten-like molecules in crystals of the Bence-Jones dimer (Edmundson et al., 1974). We now consider whether such induced changes in the combining sites may also lead to alterations in distal parts of the molecules (for discussions of this subject in functional antibodies, see Schur and Christian, 1964; Warner and Schumaker, 1970; Hyslop et al., 1970; Holowka

† From the Division of Biological and Medical Research, Argonne National Laboratory, Argonne, Illinois 60439, and the Departments of Biochemistry and Biology, University of Utah, Salt Lake City, Utah 84112. *Received May 13, 1977.* This work was supported by the U.S. Energy Research and Development Administration and by U.S. Public Health Service Grant No. CA-19616.

‡ Present address: Department of Biochemistry, University of Utah, Salt Lake City, Utah 84112.
§ Present address: Abbott Laboratories, North Chicago, Illinois 60064.

0006-2960/78/0417-0158$01.00/0

et al., 1972; Tumerman et al., 1972; Pilz et al., 1973; Metzger, 1974; Pollet et al., 1974; Givol et al., 1974; Schlessinger et al., 1975; Cathou and Dorrington, 1975; Brown and Koshland, 1975; Jaton et al., 1975; Givol, 1976; Colman et al., 1976; Huber et al., 1976).

The binding of dinitrophenyl (Dnp)[1] groups by the Bence-Jones dimer was used as the test system. After the protein was exposed to bis(Dnp)lysine in solution, the ligand was removed and the protein was crystallized. The crystallized protein was then examined for evidence of conformational changes in the C domains after ligand binding.

Materials and Methods

Preparation of Samples. Samples of covalent dimers and noncovalent dimers with the interchain half-cystine residues modified by disulfide interchange reactions were prepared by methods given in the accompanying article (Firca et al., 1978). Noncovalent dimers were also produced by reduction and carboxymethylation of the interchain disulfide bond under nondissociating conditions (Morris and Inman, 1968). After reduction at pH 8.2 with 0.01 M 2-mercaptoethanol (ME) in 0.1 M Tris-HCl, 0.06 M NaCl, the protein was reacted at 30 °C with 0.03 M sodium iodoacetate for 2 h in the dark. The reactants were removed by dialysis against 0.02 M sodium phosphate, pH 7.4, at 4 °C. One of the products crystallized when the mixture was dialyzed at 4 °C against 0.02 M sodium acetate, pH 6.0. These crystals were harvested, redissolved, and used for subsequent crystallization experiments.

Crystallization of Dimers. To prepare trigonal crystals similar to those of the native Bence-Jones dimer (Edmundson et al., 1971), the solutions of covalent or noncovalent dimers were dialyzed at 4 °C against 0.02 M sodium phosphate, pH 7.4, and concentrated to 20–23 mg of protein per mL by ultrafiltration. Proteins were crystallized at 19 °C and at pH 6.2 in ~1.6 M ammonium sulfate which was 0.1 M in phosphate. Trigonal crystals were obtained in all cases, but bundles of needles were also observed.

Recrystallization of Needles. Bundles of needles of covalent dimers were harvested, washed with ammonium sulfate, redissolved in 0.02 M phosphate buffer, pH 7.4, and concentrated to 23 mg/mL by ultrafiltration. In an attempt to produce orthorhombic crystals (space group $P2_12_12$, with a = 72.6, b = 81.9, and c = 71.0 Å; Schiffer et al., 1970), the solution was dialyzed at 19 °C against deionized water in microdiffusion tubes (Zeppezauer et al., 1968).

A second sample of dissolved needles was dialyzed against the buffers used in the reassembly procedure (see Firca et al., 1978). The solution was then dialyzed against 0.02 M phosphate, pH 7.4, concentrated to 23 mg/mL, and recrystallized with ammonium sulfate.

Conversion of Needles to Trigonal Forms. Another sample of needles was successively dialyzed against 0.02 M phosphate, pH 7.4, and 0.1 M borate, 0.004 M EDTA, pH 8.7, and treated for an hour with 0.1 M mercaptoethylamine (MEA) to reduce the interchain disulfide bond. The resulting solution was subjected to the procedure for covalent reassembly, and the protein was crystallized in ammonium sulfate.

Twinning of Trigonal Crystals. To obtain fragments of appropriate size for diffraction experiments, "normal" trigonal crystals are cut perpendicular to the c axis on one side of the midplane. We have also observed unusual twinned crystals in which corresponding faces have mirror symmetry across this midplane. The properties of both fragments and intact crystals of the twins were studied by diffraction techniques.

Crystallization of Reassembled IgG1 Protein. The IgG1 molecules reassembled from heavy chains and Bence-Jones monomers were concentrated to 20 mg/mL and crystallized at 11 °C by dialysis against 0.01 M phosphate, pH 6.2, in microdiffusion tubes. The morphology of the crystals was compared with that of the orthorhombic form of the native protein (space group $C222_1$, with a = 87.8, b = 111.3, and c = 186.7 Å; Edmundson et al., 1970).

Crystallographic Experiments. Trigonal crystals were examined by x-ray diffraction techniques (Edmundson et al., 1971). Data were collected to 3.5-Å resolution with a Picker FACS-1 diffractometer. The results for each modified or reassembled dimer were compared with those for the native Bence-Jones protein by difference Fourier analysis. Difference maps were calculated to 6.5-Å resolution using phase angles obtained by the multiple isomorphous replacement (MIR) method. At 3.5-Å resolution, difference maps calculated with MIR phases showed "ghost" peaks in positions corresponding to heavy-atom substitution sites. The ghost peaks were absent in both the 6.5-Å MIR maps and in 3.5-Å maps calculated with refined phases. Refinement of the native protein structure was carried out with Diamond's (1971) real space refinement program (M. Schiffer et al., unpublished data). Phases used in the 3.5-Å difference maps were obtained after two cycles of refinement.

Packing of Dimers in Trigonal Crystals. Atomic coordinates measured from the model of the Bence-Jones dimer were used to construct packing diagrams for the trigonal crystals. Stereo plots were generated with the aid of Argonne and ORTEP programs (K. J. Williams, J. M. Fenton, and E. E. Abola, unpublished data; Johnson, 1976).

Crystallization of Bence-Jones Dimers after Binding of Bis(Dnp)lysine and Subsequent Removal of the Ligand. Bis(Dnp)lysine in 0.11 M sodium phosphate, pH 6.2, was bound to native Bence-Jones dimers at 4 °C by the method of equilibrium dialysis (see Figure 11 in Firca et al., 1978). A sample containing 2 mol of bound bis(Dnp)lysine per mol of protein was dialyzed against pH 6.2, 0.11 M sodium phosphate until the spectrophotometric readings at 365 nm indicated quantitative removal of ligand. The protein was concentrated to 23 mg/mL and crystallized in ammonium sulfate.

Results and Discussion

Crystal Morphology. Photographs of typical trigonal, twinned trigonal, orthorhombic, and needle forms of Bence-Jones covalent dimers are presented in Figure 1. Noncovalent Bence-Jones dimers and intermediates and end products obtained in the dissociation and reassembly of light chains of the IgG1 protein crystallized in one or more of these forms.

The trigonal form produced by the native Bence-Jones dimer in ammonium sulfate was taken as the normal case with which all other samples were compared. Needles represented the major abnormal form and were present in varying proportions in all samples of reassembled dimers and their intermediates.

Trigonal crystals predominated when Bence-Jones dimers were dissociated through noncovalent intermediates (mixed disulfides) and covalently reassembled. Needles were the only form to appear after the covalent Bence-Jones dimer was treated with acid (0.2 M acetic or 0.4 M propionic acid) and subsequently dialyzed against the reassembly buffers. Samples of light chains dissociated from heavy chains as monomers and

[1] Abbreviations used are: Dnp, 2,4-dinitrophenyl; EDTA, (ethylenedinitrilo)tetraacetic acid, disodium salt; ME, 2-mercaptoethanol; MEA, 2-mercaptoethylamine; S-CM, *S*-carboxymethyl; MAA, 2-mercaptoacetic acid; MIR, multiple isomorphous replacement.

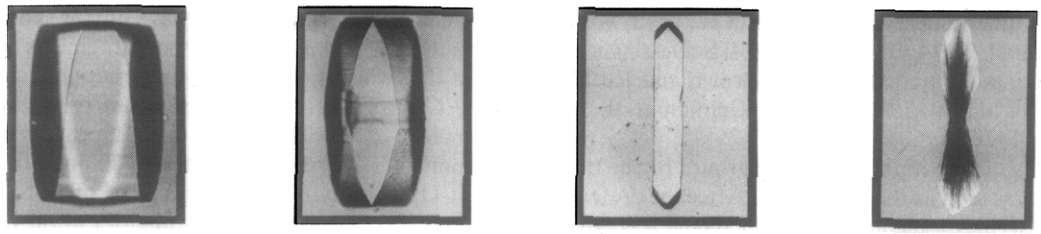

FIGURE 1: Photographs of crystals of the urinary Bence-Jones λ-chain dimer from the patient Mcg. (a) Normal trigonal form of the native Bence-Jones covalent dimer, crystallized from ammonium sulfate in the space group $P3_121$, with $a = 72.3$ and $c = 185.9$ Å. Light chains dissociated from the parent IgG1 protein and reassembled into a covalent dimer can also be crystallized in this form, as can noncovalent Bence-Jones and light chain dimers (e.g., S-CM derivatives and mixed disulfides with MAA, ME, or MEA alkyl groups). (b) Twinned trigonal form, which appears with a frequency of about 5% of the total number of crystals of the native Bence-Jones dimer. This frequency increases in dissociation and reassembly experiments and reaches values as high as ~90% in noncovalent dimers derivatized with ME groups. See Figure 3 for more detailed morphology. (c) Orthorhombic form of the native Bence-Jones dimer, crystallized by dialysis against water. The space group is $P2_12_12$, with $a = 72.6$, $b = 81.9$, and $c = 71.0$ Å. (d) Needle form of reassembled covalent Bence-Jones dimer crystallized in ammonium sulfate. This form, which is not suitable for diffraction studies, also appears in varying proportions in samples of covalently reassembled light chain dimers and in noncovalent intermediates in the dissociation and reassembly of both light chains and Bence-Jones proteins. Samples obtained by dissolving the needles have strikingly different CD spectra from constituents of the trigonal form. The spectral differences have been interpreted in terms of conformational changes, particularly in segments containing aromatic residues tryptophan-189 and tyrosine-195, which are spatially near the interchain disulfide bond (see Firca et al., 1978).

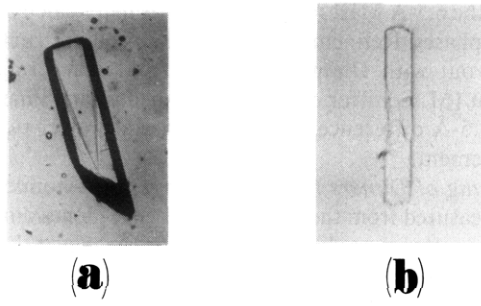

FIGURE 2: Photographs of crystals of the serum IgG1 immunoglobulin from the patient Mcg. (a) Native protein, crystallized by dialysis against water in the space group $C222_1$, with $a = 87.8$, $b = 111.3$, and $c = 186.7$ Å. (b) A crystal of the IgG1 protein reconstituted from heavy chains of the parent immunoglobulin and monomers of the urinary Bence-Jones protein. This crystal, which was prepared by dialysis against 0.01 M phosphate, pH 6.2, has the same morphology as that of the native IgG1 protein, but is too thin for diffraction studies.

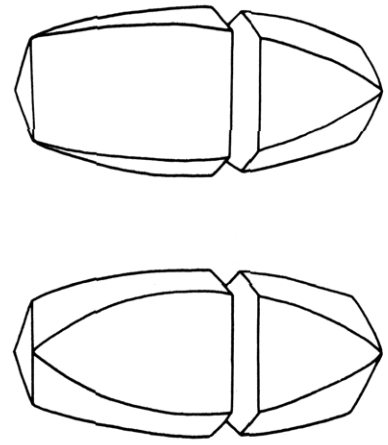

FIGURE 3: Drawing of the normal and twinned forms of trigonal crystals of the Bence-Jones dimer to show how they are cut for diffraction studies. Note the differences in the appearance of the faces of the normal (upper crystal) and twinned forms. The faces of the latter are related by a mirror plane crossing the middle of the crystal perpendicular to the long axis (c). If the entire crystal is used for diffraction, the twinning is manifest by the observation that the intensities of the hkl reflections are equal to those of the khl reflections. When the crystals are cut as in the drawing, however, the morphologies and the diffraction patterns of the fragments from the normal and twinned crystals are indistinguishable.

reassembled into covalent dimers usually had a higher proportion of needles than comparable Bence-Jones proteins.

Examination of individual stages in the dissociation and reassembly procedure showed that the noncovalent intermediates were particularly susceptible to needle formation.[2] For example, needles were produced after prolonged treatment of the intermediates with acid (0.4 M propionic acid for >24 h at 4 °C), prolonged dialysis (>4 days at 4 °C) against dilute acetate buffers, or chromatography over CM-Sephadex C-50 in either acetate or phosphate buffers.

Individual needles were too small to use for x-ray analysis. However, dissolved needles crystallized in water in a form similar to the orthorhombic crystals (see Figure 1c), and direct comparisons with the native dimer may be possible in the future.

[2] The S-carboxymethylated (S-CM) derivative represents a special case. Crystals resembling the orthorhombic form of the Bence-Jones dimer (see Figure 1) spontaneously appeared when the reaction mixture was dialyzed against the pH 6.0, 0.02 M sodium acetate buffer used for chromatographic purification of derivatives (see Firca et al., 1978). The reaction mixture contained two electrophoretic components, but the crystals were composed of a single electrophoretic species in which the carboxymethylation was probably limited to the half-cystine residues of the interchain bond (see Palmer et al., 1963). When recrystallized in ammonium sulfate, the S-carboxymethylated derivative produced a mixture of trigonal crystals and needles.

Photographs of crystals of the native IgG1 immunoglobulin and the protein reassembled from heavy chains and Bence-Jones monomers are shown in Figure 2. The appearance of crystals with the same habit in the two samples adds to the evidence that the two types of Bence-Jones isomers assume the single conformation of the IgG1 light chain when mixed with the heavy chain (see Firca et al., 1978).

Structural Implications of Trigonal and Needle Forms of the Dimers. For further studies the bundles of needles appearing in the mixtures were easily separated from trigonal crystals and washed free of mother liquor. When dissolved and recrystallized, the needle form consistently reappeared and trigonal crystals were absent. Control samples of native Bence-Jones dimers recrystallized exclusively in the trigonal form.

CD spectra of dissolved needles were markedly different from those of the native dimer in the aromatic regions (see Firca et al., 1978). When considered in conjunction with the

TABLE I: Data for Trigonal Crystals of Native and Recombinant Dimers and Derivatives, All with Space Group $P3_121$.

Crystal	Cell dimensions (Å)		R_f in shells[b]						Max peak heights[c]		Decay[e] (%)
	a	*c*	*A*	*B*	*C*	*D*	*E*	*F*			
Native BJ-S-S-BJ[a] (control)	72.3	185.9	0.040	0.049	0.039	0.043	0.063	0.068	0.28	0.06[d]	5-9
Recombinant BJ-S-S-BJ	72.4	186.4	0.060	0.069	0.078	0.062	0.075	0.073	0.43	0.08	9-10
Recombinant BJ-S-S-BJ (converted needles)	72.3	186.5	0.043	0.038	0.046	0.047	0.052	0.043	0.27	0.06	2-4
Recombinant BJ-S-S-BJ (exposed to H chains)	72.3	185.9	0.074	0.080	0.087	0.093	0.104	0.102	0.71	0.11	9-12
L-S-S-L	72.3	185.8	0.125	0.103	0.123	0.133	0.135	0.146	0.88	0.17	4-9
$(BJ\text{-}S\text{-}CM)_2$	72.3	186.5	0.133	0.138	0.162	0.107	0.129	0.111	0.75	0.15	4-6
$(BJ\text{-}S\text{-}S\text{-}MAA)_2$	72.3	186.7	0.058	0.080	0.122	0.111	0.105	0.114	0.61	0.13	4-6
$(BJ\text{-}S\text{-}S\text{-}ME)_2$	72.3	186.7	0.105	0.130	0.158	0.122	0.125	0.122	0.74	0.15	9-10
$(BJ\text{-}S\text{-}S\text{-}MEA)_2$	72.3	186.6	0.075	0.079	0.090	0.063	0.068	0.093	0.55	0.10	9-12

[a] Abbreviations: BJ-S-S-BJ, Bence-Jones dimer, covalently linked by the interchain disulfide bond; L-S-S-L, covalent dimer prepared from the light chain components of the IgG1 protein; $(BJ\text{-}S\text{-}CM)_2$, the noncovalent dimer of the *S*-carboxymethyl derivative of the Bence-Jones protein; $(BJ\text{-}S\text{-}S\text{-}MAA)_2$, the mixed disulfide dimer in which the MAA alkyl group is 2-mercaptoacetic acid; $(BJ\text{-}S\text{-}S\text{-}ME)_2$, mixed disulfide with 2-mercaptoethanol; and $(BJ\text{-}S\text{-}S\text{-}MEA)_2$, mixed disulfide with 2-mercaptoethylamine. [b] $R_f = \Sigma|F_{P'} - F_P|/\Sigma F_P$, where F = structure factor amplitude, P = native protein, and P' = recombinant or derivatized protein. The data were collected in the following shells: $A = \infty$ to 6.5 Å; B = 6.5 to 5.0 Å; C = 5.0 to 4.4 Å; D = 4.4 to 4.0 Å; E = 4.0 to 3.7 Å; and F = 3.7 to 3.5 Å. [c] These values are all on the same scale and represent the highest electron density (or the largest trough) in the 3.5-Å map. The values for the control sample were obtained by comparing two sets of data for the native Bence-Jones dimer. [d] Standard deviation, defined in footnote 3. [e] The decay is based on the average decrease in intensity of 30 general reflections from the *A* shell after 30-h exposure at 19-20 °C to Cu Kα 42 kV, 16 mA.

TABLE II: Coordinates of Centers of Representative Peaks and Troughs in 3.5-Å Difference Fourier Maps.

Crystal		*x*	*y*	*z*	Rel peak heights	Nearest structural feature
o-Chloromercuriphenol	Peak	0.609	0.256	0.158		Site C
L-S-S-L V domains	Peak	0.64	0.27	0.15	1.0	Tyr-89, monomer 1
	Peak	0.62	0.29	0.16	0.8	Pro-46, monomer 2
	Trough	0.64	0.26	0.17	0.7	Pro-46, monomer 1
	Trough	0.52	0.22	0.17	0.7	Tyr-38, monomer 2
C Domains	Peak	0.28	0.68	0.04	0.8	Thr-209, monomer 1 Glu-127, monomer 2
	Trough	0.50	0.12	0.16	0.8	Glu-164, monomer 1 Gln-171, monomer 2
S-Hg-S	Peak	0.111	0.542	0.110		Interchain disulfide bond
$(BJ\text{-}S\text{-}S\text{-}MEA)_2$[a] C domains	Trough	0.12	0.51	0.10	1.0	Ser-216, monomer 1
	Trough	0.10	0.54	0.10	0.9	Interchain disulfide bond
	Trough	0.04	0.56	0.09	0.8	Thr-213, monomer 2
	Trough	0.02	0.58	0.09	0.8	Thr-213, monomer 2
	Peak	0.98	0.61	0.08	0.9	Pro-212, monomer 2

[a] The contours for the troughs and peaks for this derivative are shown in Figure 6.

atomic model of the native dimer, the spectral differences were interpreted in terms of local conformational changes in segments containing tryptophan-189 and tyrosine-195, which are spatially near the interchain disulfide bond.

It was possible to convert needles of covalent dimers to the trigonal form, but only after cleavage and reoxidation of the interchain disulfide bond. These samples crystallized in the trigonal form more readily and yielded more regular crystals than native Bence-Jones dimers.

Light chains failing to crystallize after dissociation from IgG1 molecules as covalent dimers were also induced to form trigonal crystals if the interchain disulfide bond was broken and reformed. Finally, dissolved needles of the MEA, ME, and MAA noncovalent dimers gave rise to trigonal crystals after covalent reassembly.

The preceding observations emphasize that the crystal habits of the Mcg proteins are sensitive indicators of conformational changes, particularly in the vicinity of the interchain disulfide bond. Altered molecules appear to be locked into relatively stable, though not native conformations by the interchain bonds. Cleavage of these bonds, even in nondissociating solvents, relieves the strains and allows the domains to complete the interactions necessary for restoration of the native structure.

Twinning of Crystals. A drawing to illustrate the differences in the habits of normal and twinned trigonal crystals is shown in Figure 3. Each individual of the twin occupies approximately half of the crystal, with a mirror plane perpendicular to the *c* direction. Approximately 5% of the crystals of native Bence-Jones dimers were twinned. The proportion was increased in samples of reassembled dimers and derivatives. In the most extreme case (the ME derivative), for example, about 90% of the crystals were twins.

The effects of the twinning were readily observed in the diffraction patterns. A fragment cut from one end of a normal trigonal crystal was used as a control. Forty-eight pairs of reflections with Miller indices of *hkl* and *khl* were selected from the 3.5-Å data set for this control crystal to give large differences in intensities between members of each pair. In a twinned crystal the intensities of the *hkl* and *khl* reflections were found to be identical within the errors of the measurements (i.e., with appropriate corrections for background and absorption). Fragments cut from either end of a twinned crystal were indistinguishable from the control (see Figure 3). As the frag-

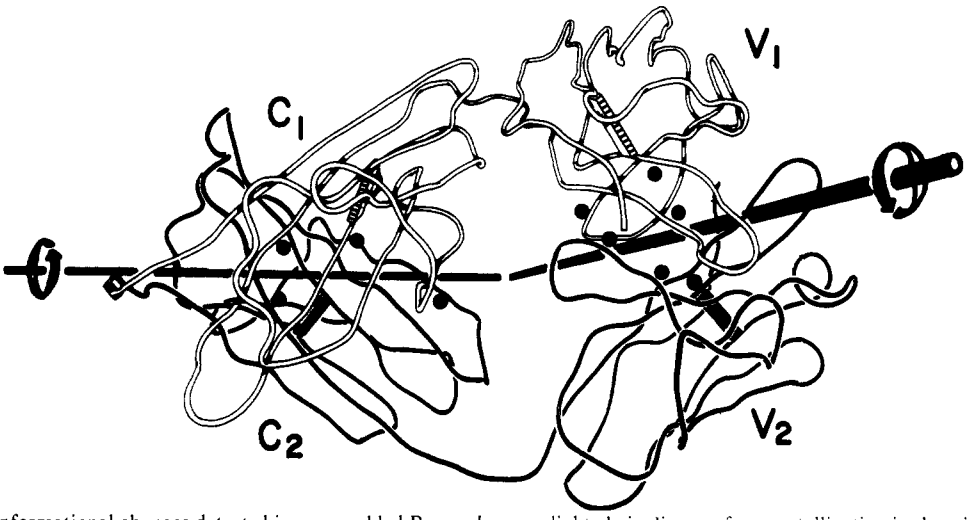

FIGURE 4: Sites of conformational changes detected in reassembled Bence-Jones or light chain dimers after crystallization in the trigonal form. These sites are marked by dots on the model of the polypeptide chains of the dimer. The white chain represents monomer 1 and the black chain monomer 2. The interchain disulfide bond is located at the far left. Local pseudo-twofold axes of rotation between pairs of like domains are superimposed on the model. The pseudo-diad between the V domains passes through the main cavity and deep pocket in which hapten-like molecules are bound. The observed conformational changes in the V domains are clustered in and around the polypeptide segments lining the deep pocket. Changes in the C_1-C_2 dimer also occur along the interface of the two domains.

ment size was increased to include portions beyond the mid-plane of the crystal, the intensities of the *hkl* reflections began to approach those of their *khl* counterparts.

The type of twinning just described is characteristic of merohedral crystal classes (Buerger, 1960). The points on the twinned lattice of the crystal are in register with those on the untwinned lattice.

Unit Cell Dimensions of Trigonal Forms of Covalent and Noncovalent Dimers. Crystal data for the dimers are summarized in Table I. The trigonal forms of covalent dimers reassembled from Bence-Jones and light chain monomers and of noncovalent dimers of S-CM, MAA, ME, and MEA derivatives all crystallized in the same space group ($P3_121$) as the native Bence-Jones protein. The unit cell dimensions also approximated those for the native protein (a = 72.3 ± 0.3; c = 185.9 ± 0.6 Å). In crystals of the S-CM, MAA, ME, and MEA derivatives, the c dimension appeared to be slightly elongated (0.4%), although the increases over the normal value were within the errors of the measurements. Dimers are aligned along c in the crystal lattice, with the interchain disulfide bond on the pseudo-twofold axis (which is only ~5° away from the c direction). The c dimension is therefore expected to be more sensitive than a to chemical modifications of the interchain disulfide.

Difference Fourier Maps for Reassembled Covalent Dimers. The difference Fourier maps were generally consistent with the chromatographic, electrophoretic, and binding studies that showed close similarities between native and reassembled covalent dimers (see Firca et al., 1978). However, the maps did reveal conformational changes along the regions of contact between the two monomers. These changes were indicated by small peaks and troughs on the maps.[3] The coordinates of representative peaks are presented in Table II. Coordinates of the site (C) occupied by *o*-chloromercuriphenol or other ligands like 5-acetyluracil and menadione are included for comparison. The locations of changes observed in various samples are indicated by dots on the photograph of the model of the Bence-Jones dimer in Figure 4.

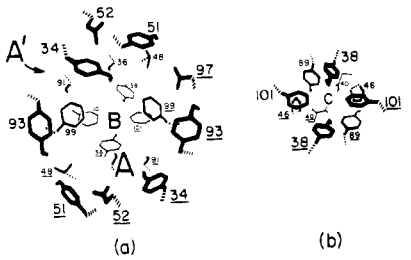

FIGURE 5: Perspective drawings of the side chains in the binding regions of the Bence-Jones dimer. Residues are numbered as in the amino acid sequence determined by Fett and Deutsch (1974). Constituents of monomer 2 are underlined, and locations of binding sites are designated by capital letters. The α-β bonds of side chains are indicated by dashed lines. (a) Lining of the main binding cavity, which is about 15 Å across at the entrance and 17 Å deep. All of the side chains are available for binding hapten-like molecules in solution, but in the crystal lattice site A' is blocked (Figures 11 and 12) and tyrosine-93 of monomer 2 is engaged in interactions with side chains from other dimers (Figure 13). Bis(Dnp)lysine bridges sites A and B in the crystals, with one Dnp ring in each site. The dimers bind two molecules of bis(Dnp)lysine in solution, with presumably one of the additional Dnp rings in site A'. (b) Lining of the deep pocket, reached through the floor of the main cavity and containing binding site C.

The most prominent peaks and troughs corresponded to the polypeptide backbones and side chains along the V domain interface, particularly the lining of site C (see Figure 5). In one sample, for example, there were positional changes of 2–3 Å in the polypeptide segment containing proline-46 and lysine-47 of monomer 2. A coupled shift of proline-46, monomer 2, and tyrosine-89, monomer 1, was found in another sample. Such shifts were not observed when difference maps for control samples of native dimers were calculated with the refined phases. The results indicate that this region of the V domain interface is particularly susceptible to distortion during the reassembly process.

Changes along the solvent-free C domain interface were

[3] To evaluate the significance level for features found in the maps, a "standard deviation," $\sigma(\rho)$, was calculated with the equation:

$$\sigma^2(\rho) = \sum_{i=1}^{N} (\rho_i - \bar{\rho})^2/(N-1)$$

where ρ_i is the electron density value at the ith grid point on the map, $\bar{\rho}$ is the overall average density value, and N is the total number of grid points. Since peaks and troughs were included in the averaging of the density values, the noise levels based on these calculations were higher than those deduced by inspection of the maps. For map features to be considered significant, we used the criterion that $|\rho_i - \bar{\rho}| \geq 3.5\sigma(\rho)$.

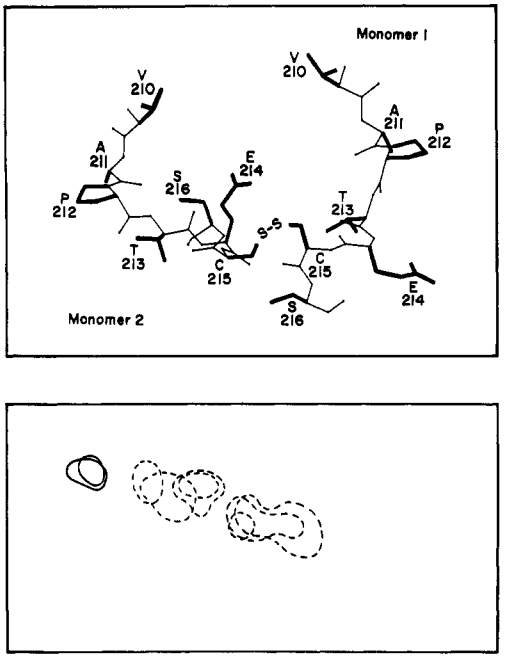

FIGURE 6: Conformational changes accompanying cleavage and chemical modification of the interchain disulfide bond. The COOH-terminal segments in the native covalent dimer are shown in the top panel with the side chains represented by the darker lines. Superposed sections of the 3.5-Å difference Fourier map for this region of the MEA noncovalent dimer are presented in the lower panel. Negative contours (dashed lines) indicate shifts in the positions of the atoms in the immediate vicinity of the disulfide bond and in the terminal peptide segment of monomer 2. The positive contours (solid lines) define the new position of proline-212 of monomer 2. The segment from the right-angled turn at proline-212 to the COOH terminus appears to recoil about 2 Å when the disulfide bond is cleaved and derivatized. Note that monomer 1, which has a different conformation around proline-212, is not appreciably altered in the MEA derivative.

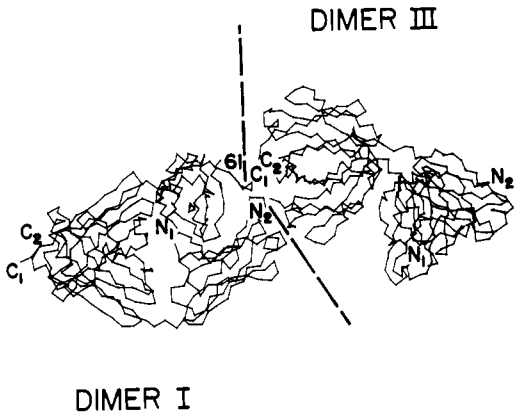

FIGURE 7: Head-to-tail arrangement of Bence-Jones dimers in the trigonal crystal lattice. The polypeptide loop containing proline-61 of monomer 1, dimer I closely approaches the C domains of another dimer (III) in the crystal lattice. The NH_2-terminal residues of monomers 1 and 2 are designated N_1 and N_2 and the COOH-terminal residues by C_1 and C_2. The interchain disulfide bond is located between C_1 and C_2 in the tracings. This packing arrangement imposes steric restrictions on the types of modifications of the disulfide bond in derivatives which are slated to be crystallized in the trigonal form. The remaining dimers in the unit cell participate in similar packing interactions. For example, dimer III approaches the C domains of dimer II, which in turn impinges on dimer I in the next unit cell. Dimers IV, V, and VI are oriented in the opposite direction from I, II, and III, but show the same kind of head-to-tail arrangement.

small and mainly involved side chains rather than polypeptide backbones (e.g., leucine-121 and phenylalanine-122). Again, the difference maps for the control samples were featureless in these regions. These results were consistent with the structural features of the native dimer. The C domains form a more compact dimeric module than the V domains (Schiffer et al., 1973), and major changes along the zone of contact would seriously interfere with dimerization during reassembly.

When trigonal crystals of the dimers showing interfacial conformational changes were dissolved and subjected to cleavage and reoxidation of the interchain disulfide bond, the proteins could be recrystallized in forms giving difference maps indistinguishable from those of control samples of native dimers. This finding suggests that the release of constraints at the carboxyl end of the molecule allows conformational readjustments of segments ~50 Å away along the V domain interface.

Difference Fourier Maps for Noncovalent Dimers. The most characteristic features of the difference maps for the noncovalent dimers (S-CM, MAA, ME, and MEA derivatives) were regions of negative electron density (troughs) in and around the position of the interchain disulfide bond in the native dimer. The coordinates for the trough minima in the MEA derivative are presented in Table II. Coordinates for the mercury atom inserted between the two sulfur atoms of the disulfide bond in an isomorphous derivative (Ely et al., 1973) are listed for comparison. Superposed sections of the difference map for the MEA derivative are shown in Figure 6.

The series of contours in Figure 6 corresponded to the positions of residues 212–215 in monomer 2. The positive contour at the left of Figure 6 was shifted about 2 Å from the position of the proline-212 ring in the native dimer. The simplest explanation for these results involves a 2-Å shift of the COOH-terminal segment of monomer 2 when the interchain disulfide bond was cleaved and derivatized. Monomer 2 makes a right-angled turn at proline-212 in the native protein, but monomer 1 has a different conformation which was not detectably changed when the disulfide bond was broken.

Implications of Crystal Packing to Permissible Modifications of Dimers. Since our test systems are dependent on the production of trigonal crystals after modifications or reassembly of the dimers, it is important to understand the steric and chemical constraints imposed by the normal interactions among dimers in the crystal lattice. These studies are directly applicable to the present problems because the major sets of crystal packing forces markedly influence the binding of hapten-like molecules, the permissible conformational changes during dissociation and reassembly, and the chemical modifications of the interchain disulfide bond.

The unit cell of trigonal crystals contains six dimers, of which the molecule depicted in this and previous publications is numbered I and given the coordinates x, y, and z. The remaining five dimers are related to molecule I with the coordinates for equivalent positions listed in the International Tables of Crystallography (space group $P3_121$, no. 152, p 257). Three dimers (I, II, and III), related by the threefold screw axis (3_1), have their V domains directed down the z axis. The three remaining dimers (IV, V, and VI) are oriented in the opposite direction. The packing interactions to be discussed involve either the above dimers or equivalent molecules in adjacent unit cells.

Interactions Involving the Carboxyl-Terminal Segments, the Interchain Disulfide Bond, and the Proline-61 Loop of Monomer 1. The head-to-tail arrangement of dimers parallel to the z axis is shown in Figure 7. The loop containing proline-61 of dimer II, monomer 1, approaches the interchain disulfide bond of dimer I (for numbering of residues in the amino acid sequence, see Fett and Deutsch, 1974). In turn,

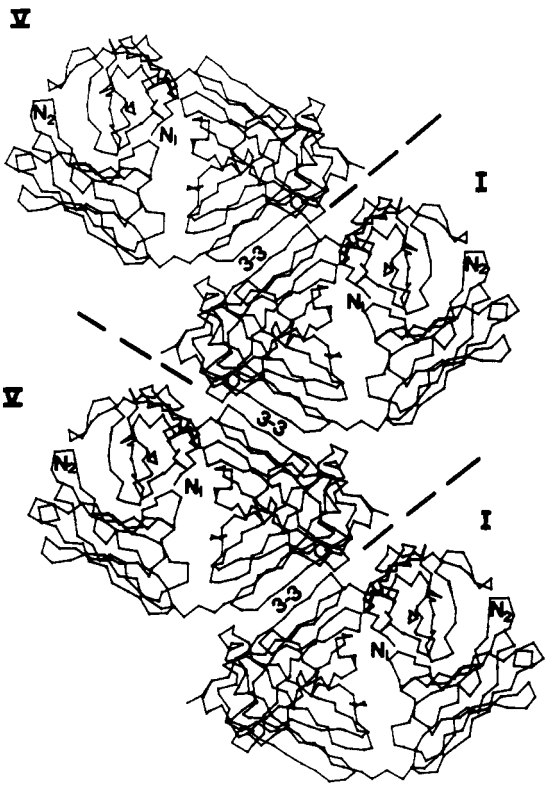

FIGURE 8: Crystal packing interactions between three-stranded β-pleated sheets of the C domains of dimers I and V. Only the αC atoms of the polypeptide chains are shown. The boundaries between adjacent dimers are marked with dashed lines, and the amino-terminal residue of each monomer is designated by N. Segment 3 of the three-stranded layer (marked 3-3) of monomer 1, dimer I, is antiparallel to its counterpart in monomer 2, dimer V. On the other side of the molecule, segment 3-3 of monomer 2, dimer I, lies opposite chain 3-3 of monomer 1 of dimer V in the adjacent unit cell. In the crystal lattice, therefore, each C domain participates in a six-stranded antiparallel β-pleated sheet across dimer boundaries. There are two other infinite arrays of dimers interacting in the same way: dimers II and VI form such an array 120° from the I–V pairs and translated by one-third of the z axis; and the array of dimers III and IV is 240° away and translated by two-thirds of the z axis.

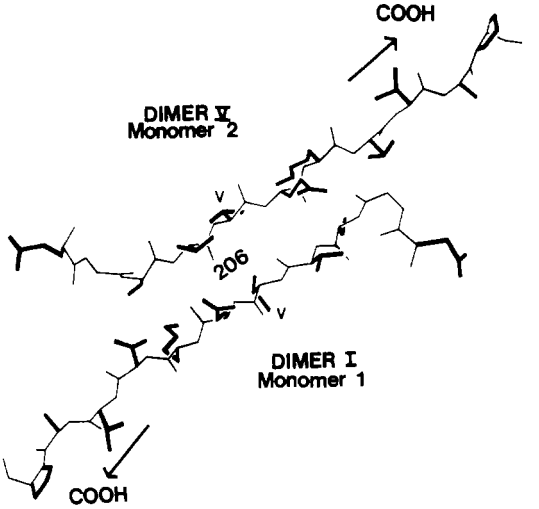

FIGURE 9: Antiparallel alignment of segments 3-3 along the dimer boundaries in the trigonal crystal lattice. The directions of the polypeptide backbones are indicated by arrows. Side chains are represented by darker lines. The orientation of the two segments is such that the valine-206 residues lie opposite each other.

dimer I, monomer 1, encroaches on the interchain linkage of dimer III, which approaches the COOH-terminal regions of dimer II in the next unit cell. The interactions resulting from the head-to-tail arrangement of dimers are weak in comparison to crystal packing forces involving the three-stranded β-pleated sheets of the C domains or the binding regions of the V domains (see following sections).

The packing diagrams show that the interchain disulfide bond of each dimer is accessible to solvent in the crystal lattice. The difference Fourier maps (Figure 6) indicate that this disulfide can be modified by the addition of one mercury atom or two S-CM, MAA, ME, or MEA groups without seriously affecting the packing. However, the close proximity of the proline-61 loop in an adjacent dimer places strict limits on the permissible changes in the conformations of the COOH-terminal segments.

Cross-Dimer Interactions between Three-Stranded β-Pleated Sheets in the C Domains. The C domains of adjacent dimers in the crystal lattice are aligned in infinite antiparallel arrays, as illustrated in Figure 8. Strand 3-3 (residues 204–211) of monomer 1, dimer I, is antiparallel to the comparable strand in monomer 2 of dimer V. The strands are aligned in such a way that the α-carbon atoms of the two valine-206 residues are opposite each other (see Figure 9). On the other side of dimer I, strand 3-3 of monomer 2 lies opposite its counterpart in monomer 1 of dimer V in the next unit cell. Thus each monomer participates in a twisted antiparallel β-pleated sheet of six strands across dimer boundaries (see Figure 10).

These arrays are the most prominent features of the crystal packing. Denaturation or modification of strand 3-3 and the remaining constituents of the three-chain layers of the C domains can seriously disrupt these arrays and thereby prevent the formation of trigonal crystals.

Interactions Involving the Binding and Switch Regions in the Crystal Lattice. The arrays of antiparallel dimers just discussed are bridged by interactions involving the binding regions of the V domains. For example, the I–V and III–IV antiparallel arrays are linked by interactions between dimers I and IV (see Figure 11). These binding region interactions contribute heavily to the stabilization of the crystal.

The switch region of monomer 2, dimer IV, passes over the binding cavity of dimer I and the side chain of leucine-110 penetrates into site A′ near tyrosine-34. Two polypeptide loops flanking the switch region, one from the V domain (leucine-14 loop in Figure 12) and one from the C domain (glutamic acid-202 loop), are separated by just enough space to interact with opposite rims of the binding cavity of dimer I.

Thus, the leucine-14 loop and the amino part of the switch region interact with rim constituents furnished by monomer 1 of dimer I, while the glutamic acid-202 loop and the carboxyl part of the switch region closely approach monomer 2 components. More specifically, the leucine-14 loop passes close to the coil containing tyrosine-32 (first "hypervariable" region) of monomer 1, and the glutamic acid-202 loop approaches the third "hypervariable" segment of monomer 2 (see Figure 12).

This region of the lattice is particularly congested. Three dimers converge so closely that their side chains engage in multiple interactions (see Figure 13). The side chains of glutamic acid-202 and lysine-114 of dimer IV (monomer 2) and of glutamine-130 of dimer III (monomer 2) are oriented toward the phenolic group of tyrosine-93 of dimer I (monomer 2). These interactions prevent the tyrosine ring from swinging into the binding cavity as a constituent of ligand site A (see Figure 5).

The above observations are important because the equivalent

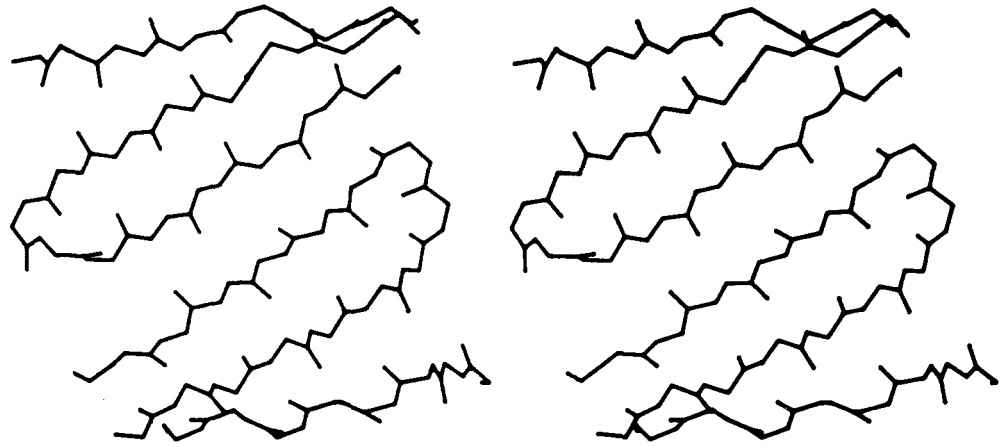

FIGURE 10: Stereo plot of the polypeptide backbones of adjacent three-stranded layers in the C domains of dimers I and V in the trigonal crystal lattice. These segments form the six-stranded antiparallel β-pleated sheets discussed in Figures 8 and 9.

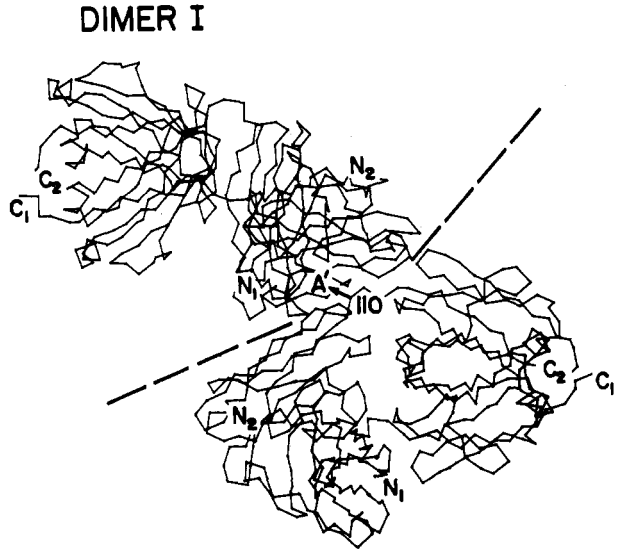

FIGURE 11: Alternate view of dimer I in the trigonal crystal lattice to show that part (site A′) of its main binding cavity for hapten-like molecules is blocked by interactions with dimer IV. The switch region between V and C domains, the leucine-14 loop from the V domain, and the glutamic acid-202 loop from the C domain of monomer 2, dimer IV, approach the binding cavity of dimer I (see Figure 12). The side chain of leucine-110 penetrates into the cavity and occupies site A′. The binding site interactions between dimers I and IV bridge the infinite arrays of I-V and III-IV pairs of dimers interacting through their three-stranded β-pleated sheets of the C domains (see Figures 8-10).

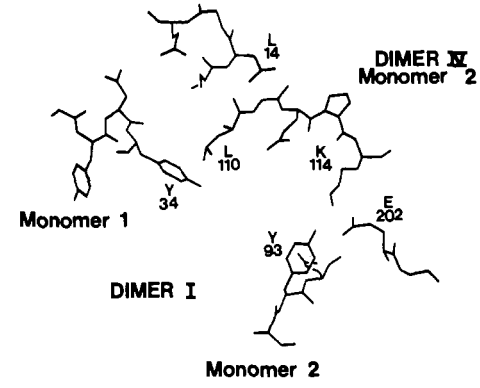

FIGURE 12: Interactions of dimer IV constituents with components of the main binding cavity of dimer I. Monomer 2, dimer IV, crosses the entry to the cavity and interacts with components on opposite rims. The leucine-14 loop and leucine-110 impinge on monomer 1 components, and the carboxyl part of the switch region (e.g., lysine-114) and the glutamic acid-202 loop closely approach monomer 2 constituents.

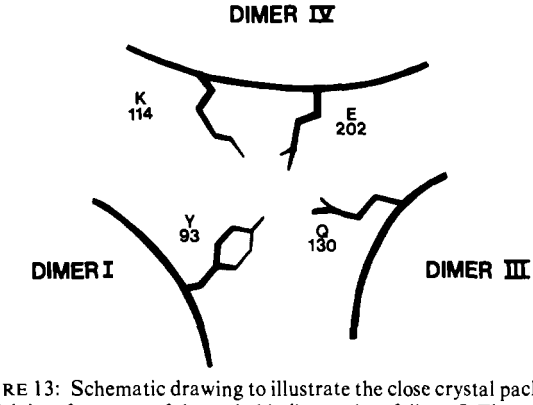

FIGURE 13: Schematic drawing to illustrate the close crystal packing in the vicinity of one part of the main binding cavity of dimer I. Three dimers approach each other sufficiently closely to permit multiple side chain interactions with tyrosine-93 of monomer 2, dimer I. The interactions with the dimer IV constituents are shown in Figure 12. The glutamine-130 residue is located in a helix at the end of the C domain of monomer 2, dimer III. These interactions prevent the side chain of tyrosine-93 from swinging into the main cavity and being a constituent of binding site A (see Figure 5).

of tyrosine-93 is involved in the binding of haptens in porcine anti-Dnp antibodies (Franěk, 1973). Fortunately for the crystal binding studies in the Mcg protein, the large entry (~15 Å across) to the cavity is only partially obstructed by the cross-dimer interactions and side chains other than the tyrosine-93 ring are available to haptens (see Figure 5). When affinity labeling is used to explore the crystal binding sites, for example, Dnp ligands can be covalently attached to the phenolic groups of tyrosines-34 and -38 of monomer 2 (Edmundson et al., 1974). Most of the remaining side chains in sites A, B, and C are also accessible for ligand binding.

Summary of the Interactions in the Crystal Lattice. The pleated sheet and binding region interactions together bridge all dimers in the unit cell. The resulting pattern is a double coiled structure around the z axis. The principal solvent channel in the crystal lattice also runs along z, and in projection appears to be surrounded by the six dimers. Three minor solvent channels, parallel to the x, y, and u axes, are confluent with the principal solvent channel. Hapten-like molecules and chemical modification agents diffuse into the crystal lattice

through these channels, which contain all of the solvent except for that inside the dimers. The solvent comprises approximately 60% of the volume of the crystal (Edmundson et al., 1971).

In the discussion of dissociation and reassembly of the dimers, we should consider the importance of conformational isomerism and rotational allomerism to trigonal packing (Edmundson et al., 1975). If the two Bence-Jones types of isomers are not formed during reassembly, the binding regions and the switch region of monomer 2 will not be in the proper orientations to provide stabilizing cross-dimer interactions. Moreover, the pronounced conformational differences in the COOH-terminal segments of the two monomers permit close head-to-tail alignment of dimers in the lattice. As a consequence of rotational allomerism the three-stranded layers face in different directions in the V and C domains. Only in the C domains are these layers external and thus available to form the cross-dimer pleated sheets that are such prominent features of the trigonal packing.

Crystal Packing of Dimer Molecules after Binding of Bis(Dnp)lysine. After removal of the two molecules of bis(Dnp)lysine bound to each dimer in solution, the protein crystallized exclusively in the needle form. Dissolved needles were converted to the trigonal forms by cleavage and reoxidation of the interchain disulfide bonds.

These results suggest that the binding of bis(Dnp)lysine in solution was accompanied by conformational changes correlated with the appearance of an abnormal needle crystal form in ammonium sulfate. The CD spectra of dissolved needles and the procedure for converting them to the normal trigonal forms indicate that the principal conformational changes in the needles have occurred in the vicinity of the interchain disulfide bond (see Firca et al., 1978). Previous binding studies with trigonal crystals showed that the binding of bis(Dnp)lysine or other ligands like menadione resulted in local conformational changes along the V domain interface, particularly around site C (see Figure 5 and Edmundson et al., 1974). The binding of a second molecule of bis(Dnp)lysine in solution, precluded by the cross-dimer interactions in the trigonal crystal lattice, would probably accentuate these local conformational changes (if the ligands occupy sites A, A′, and B as predicted from the crystal studies). Cleavage of the interchain disulfide bond apparently relieves the strains and allows reversal of both the local conformational changes in the V domains and the induced changes in the distal regions of the C domains. The mechanisms for the allosteric type effects and their reversal remain to be elucidated.

In functional antibodies the binding of antigens by the V domains can lead to the activation of complement components, with the C_H2 domain believed to bind Clq (Augener et al., 1971; Allan and Isliker, 1974; Kehoe et al., 1974; Isenman et al., 1975; Yasmeen et al., 1976; Ellerson et al., 1976). If the Bence-Jones dimer is considered a model for a primitive antibody, the results summarized in the present article can be applied to the general understanding of such induced effects in distal domains.

References

Allan, R., and Isliker, H. (1974), *Immunochemistry 11,* 175.

Amzel, L. M., Poljak, R. J., Saul, F., Varga, J. M., and Richards, F. F. (1974), *Proc. Natl. Acad. Sci. U.S.A. 71,* 1427.

Augener, W., Grey, H. M., Cooper, N. R., and Müller-Eberhard, H. J. (1971), *Immunochemistry 8,* 1011.

Brown, J. C., and Koshland, M. E. (1975), *Proc. Natl. Acad. Sci. U.S.A. 72,* 5111.

Buerger, M. J. (1960), Crystal-Structure Analysis, New York. N.Y., Wiley, p 57.

Cathou, R. E., and Dorrington, K. J. (1975), in Biological Macromolecules: Subunits in Biological Systems, Part C, Vol. 7, Fasman, G. D., and Timasheff, S. N., Ed., New York, N.Y., Marcel Dekker, p 91.

Colman, P. M., Deisenhofer, J., Huber, R., and Palm, W. (1976), *J. Mol. Biol. 100,* 257.

Davies, D. R., Padlan, E. A., and Segal, D. M. (1975), *Annu. Rev. Biochem. 44,* 639.

Diamond, R. (1971), *Acta Crystallogr., Sect. A 27,* 436.

Edmundson, A. B., Wood, M. K., Schiffer, M., Hardman, K. D., Ainsworth, C. F., Ely, K. R., and Deutsch, H. F. (1970), *J. Biol. Chem. 245,* 2763.

Edmundson, A. B., Schiffer, M., Wood, M. K., Hardman, K. D., Ely, K. R., and Ainsworth, C. F. (1971), *Cold Spring Harbor Symp. Quant. Biol. 36,* 427.

Edmundson, A. B., Ely, K. R., Girling, R. L., Abola, E. E., Schiffer, M., Westholm, F. A., Fausch, M. D., and Deutsch, H. F. (1974), *Biochemistry 13,* 3816.

Edmundson, A. B., Ely, K. R., Abola, E. E., Schiffer, M., and Panagiotopoulos, N. (1975), *Biochemistry 14,* 3953.

Ellerson, J. R., Yasmeen, D., Painter, R. H., and Dorrington, K. J. (1976), *J. Immunol. 116,* 510.

Ely, K. R., Girling, R. L., Schiffer, M., Cunningham, D. E., and Edmundson, A. B. (1973), *Biochemistry 12,* 4233.

Fett, J. W., and Deutsch, H. F. (1974), *Biochemistry 13,* 4102.

Firca, J. R., Ely, K. R., Kremser, P., Westholm, F. A., Dorrington, K. J., and Edmundson, A. B. (1978), *Biochemistry 17* (preceding paper in this issue).

Franěk, F. (1973), *Eur. J. Biochem. 33,* 59.

Givol, D. (1976), in Receptors and Recognition, Series A, Vol. 2, Cuatrecasas, P., and Greaves, M. F., Ed., London, Chapman and Hall, p 1.

Givol, D., Pecht, I., Hochman, J., Schlessinger, J., and Steinberg, I. Z. (1974), *Prog. Immunol., Proc. Int. Congr. Immunol., 2nd 1,* 39.

Holowka, D. A., Strosberg, A. D., Kimball, J. W., Haber, E., and Cathou, R. E. (1972), *Proc. Natl. Acad. Sci. U.S.A. 69,* 3399.

Huber, R., Deisenhofer, J., Colman, P. M., Matsushima, M., and Palm, W. (1976), *Nature (London) 264,* 415.

Hyslop, N. E., Jr., Dourmashkin, R. R., Green, N. M., and Porter, R. R. (1970), *J. Exp. Med. 131,* 783.

Isenman, D. E., Dorrington, K. J., and Painter, R. H. (1975), *J. Immunol. 114,* 1726.

Jaton, J.-C., Huser, H., Braun, D. G., Givol, D., Pecht, I., and Schlessinger, J. (1975), *Biochemistry 14,* 5312.

Johnson, K. C. (1976), Oak Ridge National Laboratory Report, ORNL-5138, third revision.

Kehoe, J. M., Bourgois, A., Capra, J. D., and Fougereau, M. (1974), *Biochemistry 13,* 2499.

Metzger, H. (1974), *Adv. Immunol. 18,* 169.

Morris, J. E., and Inman, F. P. (1968), *Biochemistry 7,* 2851.

Padlan, E. A., Davies, D. R., Rudikoff, S., and Potter, M. (1976), *Immunochemistry 13,* 945.

Palmer, J. L., Nisonoff, A., and Van Holde, K. E. (1963), *Proc. Natl. Acad. Sci. U.S.A. 50,* 314.

Pilz, I., Kratky, O., Licht, A., and Sela, M. (1973), *Biochemistry 12,* 4998.

Poljak, R. J., Amzel, L. M., Chen, B. L., Phizackerley, R. P., and Saul, F. (1974), *Proc. Natl. Acad. Sci. U.S.A. 71,* 3440.

Pollet, R., Edelhoch, H., Rudikoff, S., and Potter, M. (1974), *J. Biol. Chem. 249,* 5188.
Schiffer, M., Hardman, K. D., Wood, M. K., Edmundson, A. B., Hook, M. E., Ely, K. R., and Deutsch, H. F. (1970), *J. Biol. Chem. 245,* 728.
Schiffer, M., Girling, R. L., Ely, K. R., and Edmundson, A. B. (1973), *Biochemistry 12,* 4620.
Schlessinger, J., Steinberg, I. Z., Givol, D., Hochman, J., and Pecht, I. (1975), *Proc. Natl. Acad. Sci. U.S.A. 72,* 2775.
Schur, P. H., and Christian, G. D. (1964), *J. Exp. Med. 120,* 531.
Segal, D. M., Padlan, E. A., Cohen, G. H., Rudikoff, S., Potter, M., and Davies, D. R. (1974), *Proc. Natl. Acad. Sci. U.S.A. 71,* 4298.
Tumerman, L. A., Nezlin, R. S., and Zagyansky, Y. A. (1972), *FEBS Lett. 19,* 290.
Warner, C., and Schumaker, V. (1970), *Biochemistry 9,* 451.
Yasmeen, D., Ellerson, J. R., Dorrington, K. J., and Painter, R. H. (1976), *J. Immunol. 116,* 518.
Zeppezauer, M., Ecklund, H., and Zeppezauer, E. S. (1968), *Arch. Biochem. Biophys. 126,* 564.

Factors Affecting the Adenosine Triphosphate Induced Release of Iron from Transferrin†

Franklin J. Carver and Earl Frieden*

ABSTRACT: The release of iron from transferrin was investigated by incubating the diferric protein in the presence of potential iron-releasing agents. The effective chemical group appears to be pyrophosphate, which is present in blood cells as nucleoside di- and triphosphates, notably adenosine triphosphate (ATP). An alternative structure with comparable activity is represented by 2,3-diphosphoglycerate. Neither 1 mM adenosine monophosphate (AMP) nor 1 mM orthophosphate released iron from transferrin. The ATP-induced iron-releasing activity was dependent on weak acidic conditions and was sensitive to temperature and sodium chloride concentration. The rate of iron release rapidly increased as transferrin was titrated with HCl from pH 6.8 to 6.1 in the presence of 1 mM ATP and 160 mM NaCl at 20 °C. Iron release from transferrin without ATP was observed below pH 5.5. Ascorbate (10^{-4} M) reduced Fe(III), but only after iron release from transferrin by a physiological concentration of ATP. A proposal for the mechanism of iron release from transferrin by ATP and the utilization of reduced iron by erythroid cells is described.

Transferrin is the major vertebrate iron transport protein, having a high stability constant for iron on the order of 10^{24} M^{-1} (Aasa and Aisen, 1968; Aasa et al., 1963). In serum the high avidity of transferrin for iron is especially necessary since ferric ion is insoluble at physiological pH. Iron binding is maintained by six metal ligands for each of two sites per molecule of transferrin (Aisen and Brown, 1977). These ligands include the phenolic group of two-three tyrosine residues, the imidazole group of one-two histidine residues, the anionic ligand site (usually filled by carbonate or bicarbonate), and at least one water molecule (Aisen and Brown, 1977).

When transferrin binds to erythropoietic cells, the binding affinity of the transferrin-iron(III) complex is lowered and iron released for heme synthesis. In order to lower the binding affinity of the transferrin-iron(III) complex it may be necessary to protonate one or more of the iron ligands and/or completely dissociate the carbonate (bicarbonate) from the anionic site. It has been suggested that bicarbonate release is a prerequisite for iron release from transferrin in both in vitro and cell-free systems (Aisen and Leibman, 1973; Egyed, 1973, 1975; Martinez-Medellin and Schulman, 1973).

For several years our laboratory has been interested in problems related to the mobilization of iron from transferrin by immature erythroid cells from the bullfrog, tadpole, and rabbit (James and Frieden, 1975; James, 1976; Carver and Frieden, unpublished results). Recent studies have concentrated on the effects of small molecular weight chelators and reducing agents directly on transferrin (Carver and Frieden, 1977). Of particular interest are the nucleotides which are present as iron ligands (i.e., adenosine and guanosine triphosphates) in reticulocytes and mature red blood cells (Bartlett, 1976a,b; Goucher and Taylor, 1961; Konopka et al., 1969; Konopka and Szotor, 1972). The chemical properties of the ATP-Fe(III) complex have been investigated (Goucher and Taylor, 1965; Neuberg and Mandl, 1949). ATP as well as other potential trivalent chelators, such as citrate, have the capacity to exchange iron between transferrin molecules (Aisen and Leibman, 1968; Donovan et al., 1976; Morgan, 1977) and from transferrin to ferritin (Miller and Perkins, 1969; Mazur et al., 1960). ATP is abundant (~2 mM) in immature and mature red blood cells (Bartlett, 1976a,b; Brown et al., 1972) compared to other potential and effective biological trivalent iron chelators.

The present study was undertaken to determine the role of ATP and other nucleotides in the release of iron from transferrin and the effect of reducing agents on free and protein-bound iron. It was necessary to use weak acidic conditions to evaluate the effects of potential iron-releasing agents on transferrin.

Methods and Materials

Chemicals. All chemicals used were reagent or analytical grade.

† From the Department of Chemistry, Florida State University, Tallahassee, Florida 32306. *Received July 28, 1977.* This work was supported by National Science Foundation Grant No. GB42379 and National Institutes of Health Research Fellowship AM05408-02.

0006-2960/78/0417-0167$01.00/0